14th International Particle Accelerator Conference,Venice, Italy JACoW Publishing
ISBN: 978-3-95450-231-8 ISSN: 2673-5490 doi: 10.18429/JACoW-IPAC2023-MOPA102

DESIGN OF THE NEW 18 MeV ELECTRON INJECTION LINE FOR AWAKE Run2c

V. Bencini[1]*, F.M. Velotti , CERN, Geneva, Switzerland
[1] also at John Adams Institute for Accelerator Science, Oxford, United Kingdom

Abstract

The Advanced Wakefield Experiment (AWAKE) has demonstrated during its first run (Run1, concluded in 2018) the capability of accelerating electrons up to the energy of 2 GeV using proton driven plasma wakefield acceleration. AWAKE Run 2 has started and during the third phase of the program, Run 2c, which aims to demonstrate stable accelerating gradients of 0.5-1 GV/m and emittance preservation of the electron bunches during acceleration, the layout of the experiment will be modified to accommodate a second plasma cell. Among the many changes, the position of the primary 18 MeV electron beam line will be shifted. The beam line layout and optics will need, therefore, to be redesigned to fit the new footprint constraints and match the new beam requirements. This paper presents the proposed layout of the new 18 MeV line, detailing the constraints and specifications, describing the design procedure and showing the main results.

INTRODUCTION

During AWAKE Run 1, a 400 GeV proton beam extracted from the Super Proton Synchortron (SPS) at CERN was injected into a 10 m plasma cell where it underwent Seeded Self-Modulation to produce a train of micro-bunches with lengths approximately equal to the plasma wavelength [1, 2]. The main milestone accomplished was demonstrating that an 18 MeV electron beam can be accelerated up to 2 GeV using proton-driven plasma wakefield acceleration [3, 4]. The aim of AWAKE Run 2 is to demonstrate the possibility of scaling the experiment for high-energy physics, i.e. reaching higher energies while controlling the emittance growth of the accelerated electron beam [5]. The AWAKE Run 2 comprises four phases [6]. Run 2a, completed in 2022, demonstrated that the 18 MeV electron beam can be used to seed the proton bunch self-modulation with reproducible phase [7]. Run 2b, started in 2023, foresees the replacement of the plasma source, introducing a plasma density step to improve the efficiency of the acceleration process. Run 2c will see the installation of a second plasma source and a new 150 MeV electron line to separate the self-modulation and the acceleration stages for improved emittance preservation. Finally, Run 2d will aim to demonstrate the scalability of the experiment to longer plasma cells and higher energies. For Run 2c, the whole experiment will shift 40 m downstream in the AWAKE tunnel, resulting in significant modification of the 18 MeV electron line (Fig. 1). In this paper, we discuss the new layout and the modifications to the optics necessary to satisfy the experimental requirements.

* vittorio.bencini@cern.ch

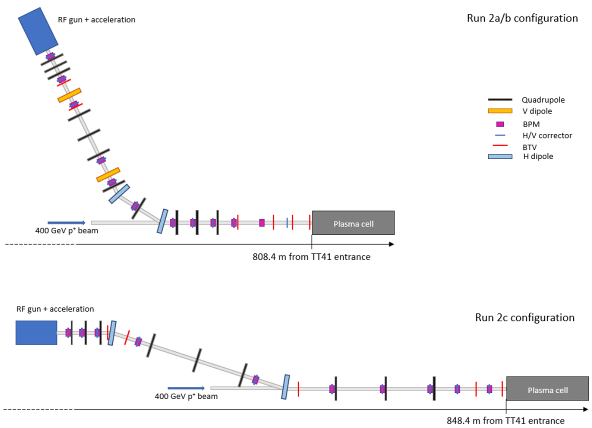

Figure 1: Layout of the 18 MeV seeding electron line in the present configuration (Run2a/b) and in the configuration foreseen for Run2c.

Table 1: Beam Line General Parameters

Parameter	Value
Momentum (MeV/c)	18
Rep. rate (Hz)	10
Bunch length (z) [ps (mm)]	4 (1.2)
Relative momentum spread $\Delta p/p_0$ (%)	0.5
Emittance (r.m.s. norm.) (mm mrad)	2

ELECTRON BEAM LINE LAYOUT

The geometry of the beam line is imposed by the constraints of the AWAKE tunnel. The purpose of the presented work is to re-design the beam line using the same magnets, power converters and beam instrumentation that are presently installed on Run2a/b 18 MeV witness line, to minimise the cost. The list and specifications of the elements used can be found in [8]. The main beam parameters of the beam line are listed in Table 1.

The main difference between the present and the new line is that the S-band, RF photo-cathode gun and the traveling wave booster linac that feed electrons to the beam line [9] will be installed on the same plane as the proton line (TT41) that transports protons to the experiment. This allows to remove the vertical dogleg and highly simplify the optics design.

The new beam line will be divided into three sections. A dispersion-free matching section, an horizontal dogleg, and a matching section where the proton and electron beam propagate coaxially before entering the plasma source.

ISBN: 978-3-95450-231-8 ISSN: 2673-5490 doi: 10.18429/JACoW-IPAC2023-MOPA102

The beam line in composed of 9 quadrupoles (of 11 available), 2 dipoles (of 4 available), 11 correctors (of 11 available), 11 BPMs (of 11 available) and 4 BTV screens (of the 6 available). The unused elements will serve as spares.

Beam Line Design Optimisation

The beam transport simulations were performed using CPyMad [10], a Cython binding to MADx [11] that gives full control and access to a MAD-X interpreter in Python. This allows to combine MADx optics simulations with Python external optimisation libraries.

The beam line design can be seen as an optimisation problem [12] with 9 bounded variables (the strengths of quadrupoles, limited by their maximum and minimum currents) and an objective function defined as follows:

$$f_{obj} = w_1(\sigma_x - \sigma_{x,t}) + w_2(\sigma_y - \sigma_{y,t}) + w_3(\alpha_x - \alpha_{x,t}) + w_4(\alpha_y - \alpha_{y,t}) + \cancel{+w_5(D_x - D_{x,t})} + \cancel{w_6(D_y - D_{y,t})}$$

where $\sigma_{x,y}$, $\alpha_{x,y}$, and $D_{x,y}$ are the beam size, the Twiss parameter α and the dispersion at the optimisation target point (namely, the plasma merge). The subscript t stands for target and represents the target values for optimisation. $w_{1,...,6}$ are the weights assigned to each term. The problem can be simplified by freezing the strengths of the two symmetric quadrupoles in the dogleg to the values that close the dispersion and removing the dispersion from the objective function. A genetic algorithm was chosen as the optimisation algorithm (in particular, the implementation of pyMOO GA [13]). The beam envelopes and dispersion functions along the line resulting from the optimisation are shown in Fig. 2.

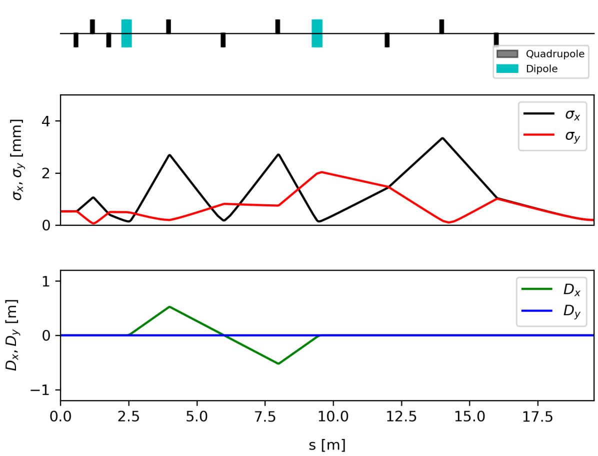

Figure 2: Matched beam envelopes and dispersion functions for the new beam line design.

The resulting optics comprises an achromatic dog-leg and symmetric optics functions at plasma cell entrance. The beam parameters at the plasma merge match the requested ones, as shown in Table 2.

Table 2: Specification and Design Beam Parameters at Plasma Merge

Parameter	Specification	Design
$\sigma_{x,y}$ (μm)	200,200	193.2,197.3
$\alpha_{x,y}$	0	0
$\beta_{x,y}$ (m)	0.705	0.676/0.704
$D_{x,y}$ (m)	0	0

ERROR STUDY

Beam Size and Position Jitter

Beam stability at injection is a key parameter to be considered for the success of Run2c. The beam central position and beam size jitter can have a considerable impact on the quality of the self-modulation process. There are mainly two sources of jitter; the fluctuations in the magnetic fields of quadrupoles, dipoles, and correctors, and the jitter of the beam generated in the acceleration section. This two factors can be included in simulations to study the effects on the beam at the plasma entrance.

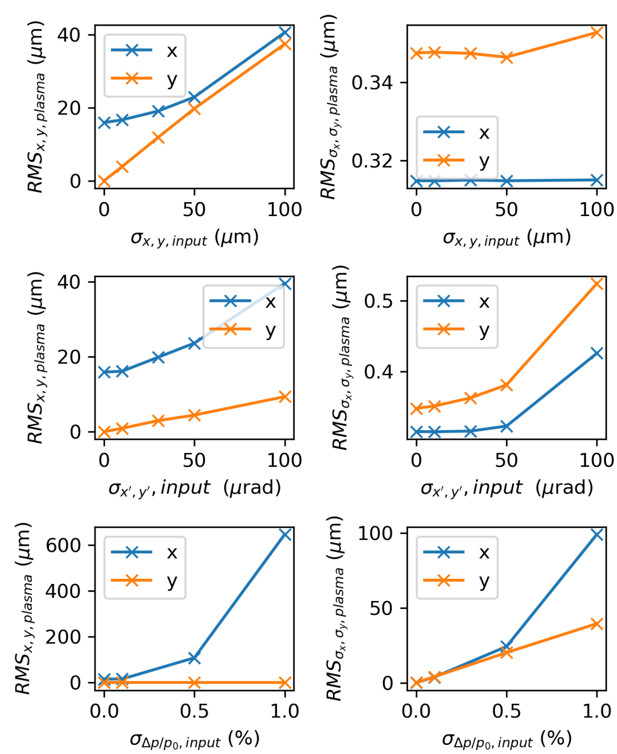

Figure 3: RMSE of beam position (left column) and beam size (right column) jitter at the plasma merge as a function of input beam central position (first row), angle (second row), and relative momentum jitter.

Since the power converters used for the new line will be the same as those installed in the current 18 MeV line, the field stability is taken as a constant input and is equal to 100 ppm [8].

ISBN: 978-3-95450-231-8 ISSN: 2673-5490 doi: 10.18429/JACoW-IPAC2023-MOPA102

The beam produced by the injector is not yet defined, as different scenarios for the upgrade of the high power RF system and of the laser are under investigation. In order to choose among the possible scenarios, it is important to assess how the input beam stability affects the beam at the plasma entrance. To do so, an error study was performed considering the effects of a set of different position $\sigma_{x,y}$ (from 0 to 100 µm), angle $\sigma_{x',y'}$ (from 0 to 100 µrad), and reference momentum jitters $\sigma_{\Delta p/p}$ (from 0 to 1 %). The three parameters were first studied separately.

For each scenario, 500 simulations were performed sampling each error from a normal distribution. Figure 3 shows the results of the error study. The position jitter is nonzero in the horizontal plane also for zero input jitter, due to the field ripple in the bending magnets. The input position and the angular jitter have a negligible effect on the output beam size jitter (<0.5% w.r.t the nominal beam size), but they have a considerable effect on the output position jitter, which grows rapidly with it. This parameter should be kept below 10 µm to keep the jitter in the y plane below 20 µm. As clearly seen from the last row of Fig. 3, reference momentum jitter is the critical source of errors and should be kept as low as possible. As a final step for the study, a simulation with 1000 seeds was performed considering the combination of all errors together. The tolerances for the input beam jitter were set to 10 µm for x and y, to 10 µrad for x' and y' and to 0.2 % for $\Delta p/p_0$. The results are summarised in Table 3. The beam jitter at the merging point is lower than the one at the beam line entrance due to the lower beta functions. Position jitter in the horizontal plane is clearly dominated by ripple in the dipoles magnetic field.

Table 3: RMS Jitter at Plasma Merge Resulting from Combining All Error Sources

Parameter	RMS of output distribution
x (µm)	21.13
y (µm)	4.52
σ_x (µm)	8.26
σ_y (µm)	9.00

Sensitivity to Input Beam Mismatch

To guarantee optimal operation of the beam line, it is important to know how sensitive it is to errors in the Twiss parameters at the its entrance. A scan was performed to quantify the effects of such errors on the output beam distribution. The study was carried out assuming no coupling between the horizontal and vertical planes and therefore treating the two separately. Values of $\alpha_{x,y}$ between -2 and 2 (symmetric with respect to nominal $\alpha_{x,y,ref} = 0$) and $\beta_{x,y}$ between 2 and 8 (symmetric with respect to nominal $\beta_{x,y,ref} = 5$) were selected. The relative percentage error $(\sigma_{x,y} - \sigma_{x,y,ref} / \sigma_{x,y,ref})$ between the simulated and the nominal beam size and the distance between the simulated focal point position and the nominal one $(s_{focus,x,y} - s_{focus,x,y,ref})$ were chosen as figures of merit to assess the impact of the initial mismatch on the output beam distribution.

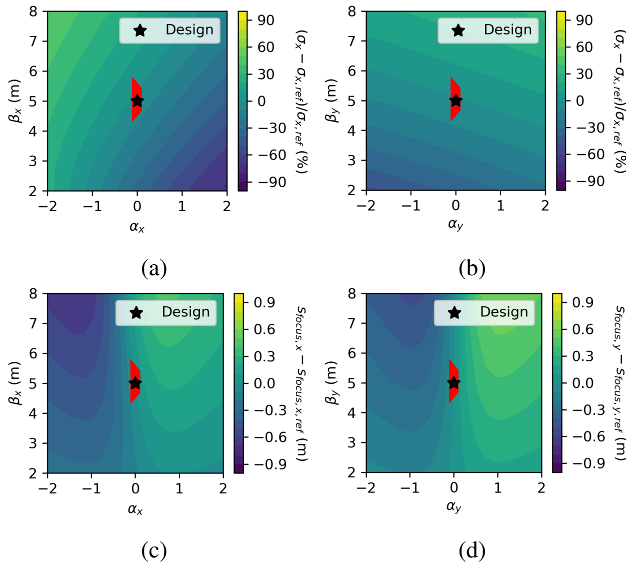

Figure 4: Results of the scan of the input Twiss $\alpha_{x,y}$ and $\beta_{x,y}$. (a) and (b) show the relative output beam size change in x and y respectively. In (c) and (d) the change in focal point position w.r.t the nominal case is shown. In red, the region where the input beam errors are acceptable. The black star corresponds to the nominal input Twiss parameters.

The result of the parameters scan is shown in Fig. 4. In Fig. 4a and Fig. 4b the relative beam size variation w.r.t. the design value as a function of the input beam Twiss parameters for the horizontal and vertical planes are shown, respectively. Figure 4c and Figure 4d show the shift of the beam waist position w.r.t. the nominal one (plasma merge). The set of input parameters resulting in an output beam with a relative beam size change within ±10 % and a shift in waist lower than ±10 cm are highlighted in red. This region defines the acceptable input beam mismatch range. The study shows that the mismatch of the beam at the plasma merge is particularly sensitive to $\alpha_{x,y}$. This interval is useful to provide an acceptability range to aim for during the commissioning of the injector. If the Twiss parameters of the produced beam fall outside the red region, the beam line optics will need to be periodically re-matched.

CONCLUSIONS

The preliminary optics design of the new 18 MeV electron seeding line for Run 2c was developed. Error studies showed the importance to control jitter in the main elements and source. The sensitivity of the line to input beam mismatch was also quantified, providing a useful tool for estimating the resulting error on the beam at the plasma entrance. Beam instrumentation and correction requirements will be studied as a next step to complete the design of the beam line.

ISBN: 978-3-95450-231-8 ISSN: 2673-5490 doi: 10.18429/JACoW-IPAC2023-MOPA102

REFERENCES

[1] M. Turner *et al.*, "Experimental observation of plasma wakefield growth driven by the seeded self-modulation of a proton bunch," Phys. Rev. Lett., vol. 122, no. 5, p. 054801, 2019. doi:10.1103/PhysRevLett.122.054801

[2] E. Adli *et al.* (AWAKE Collaboration), "Experimental observation of proton bunch modulation in a plasma at varying plasma densities," *Phys. Rev. Lett.*, vol. 122, no. 5, p. 054802, 2019. doi:10.1103/PhysRevLett.122.054802

[3] E. Gschwendtner *et al.* (AWAKE Collaboration), "AWAKE, the advanced proton driven plasma wakefield acceleration experiment at CERN," *Nucl. Instrum. Meth. A*, vol. 829, pp. 76–82, 2016. doi:10.1016/j.nima.2016.02.026

[4] E. Adli *et al.* (AWAKE Collaboration), "Acceleration of electrons in the plasma wakefield of a proton bunch," *Nature*, vol. 561, no. 7723, pp. 363–367, 2018. doi:10.1038/s41586-018-0485-4

[5] P. Muggli for the AWAKE Collaboration, "Physics to plan AWAKE Run 2," *J. Phys. Conf. Ser.*, IOP Publishing, vol. 1596, p. 012008, 2020.

[6] E. Gschwendtner for the AWAKE Collaboration, "Awake Run 2 at CERN", in *Proc. IPAC'21*, Campinas, Brazil, May 2021, pp. 1757–1760. doi:10.18429/JACoW-IPAC2021-TUPAB159

[7] L. Verra *et al.* (AWAKE Collaboration), "Controlled growth of the self-modulation of a relativistic proton bunch in plasma," *Phys. Rev. Lett.*, vol. 129, no. 2, p. 024802, 2022. doi:10.1103/PhysRevLett.129.024802

[8] J. S. Schmidt *et al.*, "The AWAKE Electron Primary Beam Line", in *Proc. IPAC'15*, Richmond, VA, USA, May 2015, pp. 2584–2586. doi:10.18429/JACoW-IPAC2015-WEPWA039

[9] S.-Y. Kim *et al.*, "Commissioning of the electron injector for the AWAKE experiment," *Nucl. Instrum. Meth. A*, vol. 953, p. 163194, 2020. doi:10.1016/j.nima.2019.163194

[10] T. Gläßle, Y. Levinsen, and K. Fuchsberger, "Cpymad: Cython binding to mad-x," *as developed on https://github. com/hibtc/cpymad.doi*, vol. 1, p. 5281, 2014.

[11] H. Grote and F. Schmidt, "MAD-X – An Upgrade from MAD8", in *Proc. PAC'03*, Portland, OR, USA, May 2003, paper FPAG014, pp. 3497–3499. doi:10.1109/PAC.2003.1289960

[12] R. Ramjiawan *et al.*, "Design and operation of transfer lines for plasma wakefield accelerators using numerical optimizers," *Phys. Rev. Accel. Beams*, vol. 25, p. 101602, 2022. doi:10.1103/PhysRevAccelBeams.25.101602

[13] J. Blank and K. Deb, "Pymoo: Multi-objective optimization in python," *IEEE Access*, vol. 8, pp. 89497–89509, 2020. doi:10.1109/ACCESS.2020.2990567